Polymer-Based Composites for Electromagnetic Shielding Application

Subjects: Polymer Science

Contributor: Yuqi Wang , Wei Zhao , Linli Tan , Yingru Li , Liu Qin , Shidong Li

Traditional metals and alloys are often used for electromagnetic interference (EMI) shielding due to their excellent electrical conductivity. However, they have drawbacks such as being heavy, expensive, and having low corrosion resistance, which limits their application in electromagnetic shielding. Therefore, it is crucial to develop novel EMI shielding materials. Polymers, being highly flexible, corrosion-resistant, and possessing high specific strength, are frequently employed in electromagnetic shielding materials.

conductive polymer composites electromagnetic shielding

1. Introduction

With the rapid advancement of electronic communications and wearable technology in the 5G era [1][2][3], people's daily lives and productivity have been greatly enhanced. However, this technological progress has also led to a new environmental challenge—electromagnetic radiation pollution, which has raised significant concerns [4][5][6]. Alongside air pollution, noise pollution, and water pollution, electromagnetic radiation pollution has emerged as another major environmental issue [7][8]. Numerous studies have demonstrated that electromagnetic radiation not only disrupts the normal functioning and reduces the longevity of electronic devices but also poses health risks, including the development of various diseases [9][10]. Therefore, whether it is to maintain the normal operation of electronic devices or to protect human health, the study of electromagnetic shielding materials has become a focus of research in recent years [11][12][13]. Metals were initially employed as electromagnetic shielding materials due to their exceptional electrical conductivity [14][15][16], but their disadvantages are also obvious. First of all, metal materials have high density, are not easy to process, and have poor corrosion resistance. Secondly, metal materials mainly shield electromagnetic waves through reflection, which will inevitably cause secondary pollution [17][18][19][20]. These shortcomings limit the application of metal materials in electromagnetic shielding. High-entropy alloys (HEAs) are expected to break the limitations of traditional alloys in the field of electromagnetic shielding. HEAs have excellent mechanical properties, corrosion resistance, and oxidation resistance. These characteristics make HEAs effective electromagnetic shielding materials in extreme environments. In addition, since HEAs are composed of multiple elements, their lattice distortion will lead to a decrease in electrical conductivity, which may change the electromagnetic shielding mechanism of the material from reflection to absorption, thereby reducing the secondary pollution caused by reflection [21][22][23][24][25]. Polymers have attracted extensive attention due to their light weight, good processability, corrosion resistance, and low cost. Researchers are gradually developing

polymers as electromagnetic shielding materials [26][27][28]. According to their components and composition, conductive polymer-based EMI shielding materials can be further separated into intrinsic and composite groups.

ICPs (Intrinsically Conductive Polymers) are a class of polymer materials with conjugated π bonds. They include PA (polyacetylene), PANI (polyaniline), PT (polythiophene), and PPy (polypyrrole). After doping, carriers are generated between polymer chains, making them conductive. These materials possess high conductivity, as well as the advantages of light weight, corrosion resistance, and good flexibility of polymer materials [29][30]. However, achieving high conductivity often requires doping, which involves complex preparation processes and high costs. Consequently, they are primarily used in special situations, such as military applications [31]. In contrast, CPCs (Conductive Polymer Composites) offer more advantages. Although the polymers used in CPCs are not conductive, they can be blended with conductive fillers to prepare lightweight, corrosion-resistant, low-cost, and processable electromagnetic shielding materials, allowing for greater flexibility in design [32][33]. Nevertheless, the characteristics of CPCs also present challenges. Increasing the content of conductive filler is necessary to improve the electromagnetic interference shielding effectiveness (EMI SE) of CPCs. However, excessively high filler content can compromise the mechanical properties and processability, and increase production costs. [33][34][35]. To address these issues, researchers have focused on enhancing the structure of CPCs, including foam structures [36][37][38], separated structures [39][40], and layered structures [41][42][43]. These improved CPCs with enhanced structures exhibit superior electromagnetic shielding capabilities and have gained widespread application. Presently, research on CPCs has become a popular topic, especially with the rapid advancement of 5G communication technology and the potential future prospects of 6G technology. As a result, CPCs will play a significant role in the development of EMI shielding technology [44][45][46].

2. Electromagnetic Shielding Mechanism

The principle of electromagnetic interference (EMI) shielding refers to the ability of EMI materials to absorb, reflect, or weaken electromagnetic waves [47]. There are several theoretical explanations for the electromagnetic shielding process, including the eddy current effect theory, the electromagnetic field theory, and the transmission line theory. The transmission line theory is widely recognized due to its simplicity in calculation, high precision, and ease of understanding. **Figure 1** illustrates the specific mechanism [48]. When an electromagnetic wave travels through a material, a portion of the wave is reflected on the surface of the electromagnetic shielding material caused by a discontinuity in the interface impedance (i.e., reflection loss efficiency, SE_R). A part of the electromagnetic wave enters the material and is continuously attenuated due to loss (i.e., absorption loss efficiency, SE_A). A portion of the electromagnetic wave will be dissipated by multiple reflections inside the material (i.e., multiple reflection efficiency, SE_M), and the remaining electromagnetic waves will be transmitted in waves after passing through the shielding material. The shielding performance of a material is usually expressed by the shielding efficiency (SE), which can be expressed by Equation (1) [49][50][51][52].

$$SE = SE_R + SE_A + SE_M \quad (1)$$

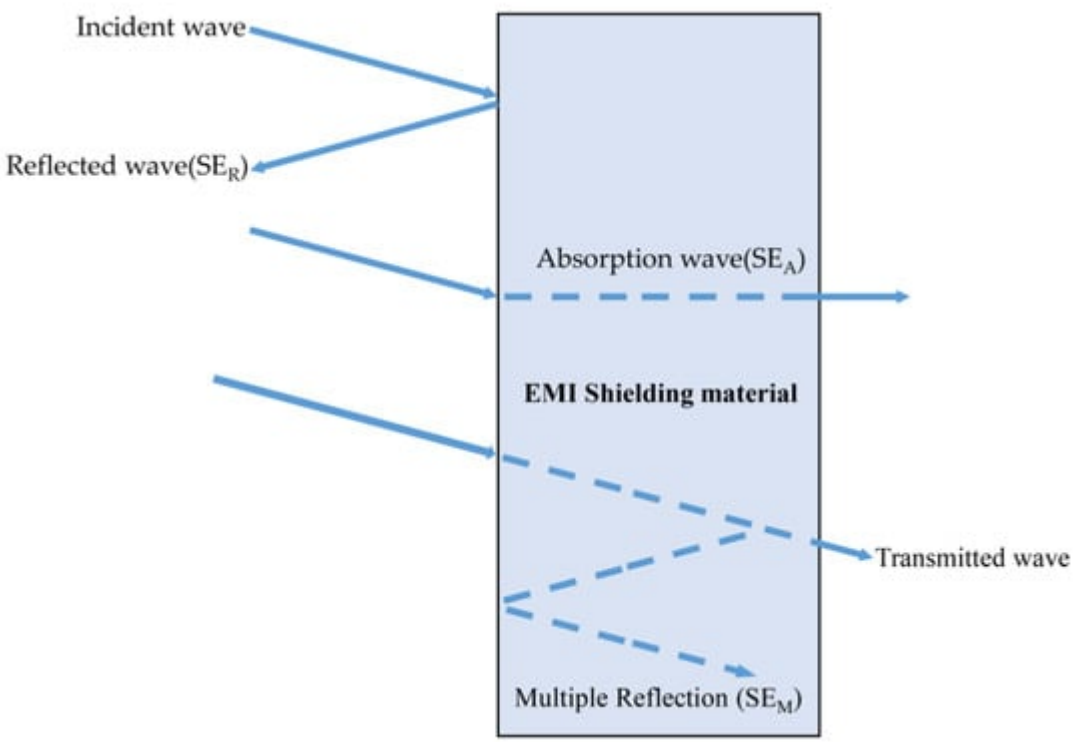

Figure 1. Electromagnetic shielding mechanism diagram.

EMI SE is strongly associated with the charge, current, and polarization events occurring on the surface and inside the shielding enclosure [53][54]. When an electromagnetic wave is reflected and absorbed by the shielding surface, there is poor impedance matching between the shielding material surface and the free interface, resulting in induced charges in the magnetic field within the shielding material. Therefore, it is necessary for the shielding material to have good conductivity [55][56]. Conductivity is a crucial factor influencing the electromagnetic shielding ability of materials, since higher conductivity generates a larger number of free charges, leading to impedance mismatch and increased reflections. Increased reflection results in a higher SE_R of the material, subsequently increasing the SE of the material as well [57][58]. When an un-reflected electromagnetic wave enters the shielding material and is absorbed and attenuated, the material contains numerous dipoles that experience orientation polarization within the magnetic field. Hence, the shielding material must possess good magnetic conductivity, excellent electromagnetic loss, and an appropriate dielectric constant [59][60][61][62]; when the remaining electromagnetic wave reaches the transmission edge of the electromagnetic shielding enclosure, it undergoes multiple reflection attenuation. Shielding materials with a porous structure and a large number of interfaces can improve the frequency of multiple reflections and scatterings, thereby effectively enhancing the SE of the materials [63][64][65]. Consequently, an effective electromagnetic shielding material should exhibit both strong reflectivity and efficient electromagnetic wave absorption [66][67].

3. Research Progress of Polymer-Based Composites with Different Structures in the Field of Electromagnetic Shielding

Polymer-based EMI shielding materials have gained significant attention as a viable alternative to traditional metal materials. This is because conventional metals lack corrosion resistance and possess drawbacks such as difficult processing, heavy weight, poor air permeability, high price, and limited control over shielding effectiveness. Consequently, the use of traditional metals is restricted within certain applications [68][69]. Polymer-based materials offer several advantages, including lightweight properties, corrosion resistance, and ease of manufacturing. Moreover, for CPCs, an effective structure (conductive network) provides exceptional conductivity and ultra-high EMI shielding effectiveness. The prevailing polymer-based EMI shielding composites encompass uniform structure, isolation structure, porous structure, and layered structure [33][34][35].

3.1. Uniform Structure

The uniform structure refers to the dispersion of conductive filler in the matrix in a uniform manner. Common methods for preparing EMI shielding materials with such a structure include solution and melt blending, as well as in situ polymerization. These methods are preferred due to their low cost and simplicity. However, this type of material has a significant drawback. To enhance the EMI shielding effectiveness (SE), it is necessary to increase the filler content in the matrix. This, in turn, leads to a high percolation value of the material, ultimately impacting its mechanical properties [70][71][72][73]. Acharya et al. [74] prepared PVDF(polyvinylidene fluoride)/RGO(reduced graphene oxide) electromagnetic shielding composite; when the concentration of the material was 21%, the EMI SE reached 60 dB. Li et al. [75] obtained a POM(polyformaldehyde)/MWCNT(multi-carbon nanotube) composite. The composite, with a concentration of 40%, had an EMI SE of 70 dB. They observed that the electromagnetic interference shielding effectiveness of the material was influenced by the filler content. As the filler content increased in the matrix, the EMI SE of the material improved; however, this enhancement was accompanied by a reduction in its mechanical performance [51][74]. Consequently, it was crucial to modify the filler and develop a novel process to reduce the filler content [76]. Researches on poly-based electromagnetic shielding composites with uniform structure are summarized in **Table 1**. It is worth mentioning that the frequency range of commonly used electromagnetic waves is 0 to 400 Ghz. Most of the studies on the electromagnetic shielding performance of the polymer matrix composites mentioned herein were carried out in the frequency range of 8 ∓ 12 Ghz (X-band). This preference is due to the X-band's low atmospheric attenuation rate, where gas molecules and suspended particles in the atmosphere absorb and scatter electromagnetic waves, resulting in energy attenuation. As a result, the cost of transmitting electromagnetic waves in the X-band is relatively low while maintaining a high throughput. Consequently, the X-band is widely suitable for communication satellites, aviation and marine radars, and military applications [18][77][78].

Table 1. Summary of the research on poly-based electromagnetic shielding composites with uniform structure.

Materials *	Filler Loading	EMI SE (dB)	Thickness (mm)	Frequency	Ref.
PVA/GN/Fe_3O_4	0.1 wt%	40.7	0.2	8–12 Ghz	[79]
EP/PES/MWCNT	2.9 wt%	23	2.2	8–12 Ghz	[80]
GN/CFN	20 wt%	73	2	8–12 Ghz	[72]

Materials *	Filler Loading	EMI SE (dB)	Thickness (mm)	Frequency	Ref.
VGCNF/PVDF	5 wt%	16.4	0.82	30 Khz–1.5 Ghz	[81]
PEDOT/GNP	15 wt%	18	-	8–12 Ghz	[82]
RGO/PdNi/EVA	1 wt%	30	-	8–12 Ghz	[83]
POM/MWCNT	40 wt%	45.7	0.15	8–12 Ghz	[75]
PE/PVDF/Fe_3O_4/CNT	10 wt%	26	2.6	18–26 Ghz	[84]
PLLA/MWCNT	10 vol%	23	2.5	8–12 Ghz	[85]
PVDF/RGO	21 wt%	60	1.5	8–12 Ghz	[74]
PLA/PEO/GNP	6 wt%	10.5	-	8–12 Ghz	[86]
PMMA/GNP-MWCNT	8 wt%	36	2	8–12 Ghz	[87]
PDMS/GA	12.5 wt%	52	3	4–16 Ghz	[88]
PVDF/$Ba_4CO_2Fe_{36}O_{60}$	20 wt%	83	0.12	8–18 Ghz	[89]
CF/PAA/Fe_3O_4	10 wt%	40.6	3.5	2–18 Ghz	[90]
PVDF/PANI	30 wt%	65	1	8–12 Ghz	[73]
ABS/CB/CNT	3 wt%	29	2	8–12 Ghz	[91]
PP/MWCNT	20 wt%	47	2	8–12 Ghz	[92]
BF/PANI	7 wt%	35.73	-	8–12 Ghz	[93]
PS/PANI	40 wt%	45	0.25	8–12 Ghz	[71]
CB/EMA/TPO	30 wt%	29	1	14–20 Ghz	[94]
PLA/CNT	5.6 wt%	31.1	-	8–12 Ghz	[95]
SWCNT/PANI	3 wt%	32.8	0.5	8–12 Ghz	[96]
TPU/SiAPP/SCF/Ti_3C_2Tx MXene	20 wt%	50.5	1	8–12 Ghz	[97]

* GN—graphene; PVA—polyvinyl alcohol; CFN—carbon fiber network; VGCNF—vapor-grown carbon nanofiber; PE—polyethylene; PLLA—poly (l-lactic acid); PLA—polylactic acid; PEO—poly(ethylene oxide); GA—graphene aerogel; CF—carbon fiber; PAA—polyacrylic acid; PP—polypropylene; BF—Bagasse Fiber.

3.2. Foam Structure

Shielding materials with foam structures offer numerous advantages, including anti-aging, corrosion resistance, light weight, and low cost. These materials find applications in various fields, such as aerospace, communication electronics, and military engineering [98][99][100][101]. Compared to other materials, foam-structured EMI shielding composites excel in using a small amount of conductive filler to achieve higher electromagnetic shielding performance, resulting in lower permeability values. Moreover, the hole walls on the surface provide multiple interfaces, allowing for multiple reflections and absorptions of electromagnetic radiation within the material. This property enhances the material's EMI SE and reduces pollution caused by surface reflection to some extent. There

are three primary processes used to create foam structures: physical foaming, chemical foaming, and freeze-drying [102][103][104]. **Table 2** shows the recent research progress of foam-structured electromagnetic shielding materials.

Table 2. Summary of the research on poly-based electromagnetic shielding composites with foam structure.

Materials *	Filler Loading	EMI SE (dB)	Thickness (mm)	Frequency	Ref.
TEG/PU	3 wt%	20.4	-	8–12 Ghz	[105]
EVA/PPy/AgNPs	52 wt%	107.45	2.4	8–12 Ghz	[106]
PEN/GN/CNT/Fe_4O_3	3.5 wt%	38	0.6	8–12 Ghz	[37]
TPU/Ti_3C_2Tx MXene	0.66 vol%	72.2	2	8–12 Ghz	[107]
CO_3O_4/CNT/MF	-	25.6	3	8–12 Ghz	[108]
PET/BAHT/SWCNT	2 wt%	45.7	-	8–12 Ghz	[109]
RGO/PU	5 wt%	23	-	8–12 Ghz	[110]
CMF/SiO_2/CNT	30 wt%	61.34	2	8–12 Ghz	[38]
TPU/MWCNT	2.5 wt%	44.86	-	10–14 Ghz	[111]
PVDF/CNT	8 wt%	41	1	8–12 Ghz	[112]
PS/PMMA/MWCNT	2 vol%	25.3	2	8–12 Ghz	[113]
ABS/CB:CNT	15 wt%	81.3	5	8–12 Ghz	[114]
PBS/CNT	4 wt%	24	-	8–12 Ghz	[115]
PA6/CF	22 wt%	36.6	1	18–26 Ghz	[36]
MXene/APU	22 wt%	76.2	5	8–12 Ghz	[116]
MWCNT/WPU/PVA/MCHM	40 wt%	23	2.5	8–12 Ghz	[117]
PDCPD-CNT/GN	3.5 wt%	43	3	8–12 Ghz	[118]
PEI/Ti_3C_2Tx MXene/AG	1 wt%	28	-	8–12 Ghz	[119]
PVDF/GNPs/CNT/Ni	16 wt%	19.4	1	8–12 Ghz	[120]
ABS/CNT	7 wt%	26.6	2	8–12 Ghz	[121]

* TEG—thermally exfoliated graphene; PU—polyurethane; AgNPs—Ag nanoparticles; PEN—Poly(arylene ether nitrile); MF—melamine-formaldehyde; PET—poly(ethylene terephthalate); BAHT—bis(6-aminohexyl)

3.3. Segregated Structure

The polymer itself has low electrical conductivity, necessitating the continuous addition of conductive fillers to the polymer matrix to impart conductivity. However, excessively high filler content increases costs and processing

difficulty and damages the material's mechanical properties [122][123][124]. These challenges are effectively addressed by creating polymer-based EMI shielding materials with segregated structures. The isolation structure of these materials ensures that conductive fillers are distributed only between the polymer particle interfaces, preventing them from dispersing freely throughout the matrix. This restricted distribution increases the probability of filler overlap at the interfaces and significantly reduces the percolation threshold. Consequently, even at low filler content, the composite material exhibits strong electrical conductivity and EMI shielding capability [125][126][127]. Research by numerous investigators has demonstrated that the generation of a segregated structure is advantageous for reducing the percolation threshold of the composite, while synergistic filler interactions enhance the material's shielding ability and mechanical properties [39][40][128][129][130][131]. The recent studies of segregated-structured electromagnetic shielding materials are summarized in **Table 3**. Zhang et al. [132] prepared PVDF/Fe_3O_4-RGC composite using layered electrostatic assembly and hot pressing. Wu et al. [133] obtained Fe_3O_4@PA6/MWCNT composite with layer-adding manufacturing and molding. They found that establishing a separation structure could form a complete conductive network, and adjusting the content of magnetic fillers could effectively improve the EMI SE of the composite. Yang et al. [134] obtained TPU/EG(expanded graphite)/AG(silver) composite material. The inclusion of the Ag component at just 0.58 vol% led to remarkable improvements in the syntactic foam's conductivity and EMI SE, reaching 171.2 S/m and 56.3 dB, respectively—well exceeding the minimum requirements for commercial EMI shielding. The introduction of a porous structure effectively mitigates the impedance mismatch between the surrounding air and the composite material, facilitating more incident electromagnetic waves and reducing reflectivity. The material's reflection efficiency in the X-band decreased from 99% to 31%, successfully mitigating secondary electromagnetic wave emission pollution. Additionally, the strong interfacial bonding between the filler and matrix ensures excellent compressibility recovery and shielding stability, even after 50 compression cycles. Wang et al. [135].prepared BPEI(multiblock polyetherimide)/MLG(multilayer graphene) composites. Due to the existence of two blocks with large TG differences in BPEI, the polymer has a high chain mobility, which allows it to inter-diffuse between the BPEI particle interfaces below TK-N, forming a good isolated conductive network. The findings demonstrated that the BPEI/MLG composite loaded with 5.0 wt% MLG generated an isolation structure at a temperature of 270 °C, thereby giving it an electrical conductivity of 313.5 S/m and an EMI shielding performance of 62.2 dB. Ma et al. [136] prepared a CNT/PDMS(polydimethylsiloxane) composite by establishing chemical bonds between them. The cross-linked network of PDMS microspheres prevents the penetration of CNTs into the polymer microcells, resulting in the formation of segregated structures. The results showed that even with only 2.2 vol% of CNT, this composite exhibited exceptional shielding performance at 47.0 dB. Notably, the tensile strength and elongation at break of the composite material reached 3.6 MPa and 87.0%, respectively, marking a substantial increase of 35.0 and 7.0 times compared to traditional isolation composite materials. Additionally, the material exhibited excellent reliability, retaining a high EMI SE of 80% even after undergoing 1000 strain-release cycles at 30% ultimate elongation.

Materials with a segregated structure have garnered considerable interest due to their outstanding EMI shielding performance and remarkably low percolation threshold. However, the distribution of conductive fillers at the polymer particle interface poses challenges, hindering molecular chain diffusion and affecting interface compatibility. Additionally, agglomerated conductive fillers generate micropores along the direction of the

conductive path. These adverse circumstances will impact the mechanical characteristics of the polymer-based EMI shielding material with a segregated structure [137][138][139][140]. Yang et al. [141] added SiO_2 particles to PDMS, and the EMI SE of the composite was improved due to the volume exclusion effect and multi-interface. However, nanoparticles disrupt conductive networks.

Table 3. Summary of the research on poly-based electromagnetic shielding composites with segregated structure.

Materials *	Filler Loading	EMI SE (dB)	Thickness (mm)	Frequency	Ref.
Starch/CNT	3 vol%	33.12	1.6	8–12 Ghz	[128]
PEBA/CNS composites	0.2 wt%	33	3.4	8–12 Ghz	[39]
PS/CNT/PEDOT:PSS	6 wt%	33.4	0.6	8–12 Ghz	[129]
PVDF/Fe_3O_4-RGC	2.02 vol%	44.5	-	8–12 Ghz	[132]
Fe_3O_4@PA6/MWCNT	9 wt%	24.8	0.5	8–12 Ghz	[133]
BPEI/MLG	5 wt%	62.2	2.3	8–12 Ghz	[135]
PP/RGO/MWCNT	5 wt%	16	-	8–12 Ghz	[127]
PLA/PBS/MWCNT	2 wt%	27.56	2	8–12 Ghz	[130]
PA12/CNT	5.66 wt%	23.9	2	8–12 Ghz	[131]
POM/CNT	4 wt%	21.5	2	8–12 Ghz	[40]
BN/GNP/PPS	40 wt%	70	3	8–12 Ghz	[139]
SiO_2/CNT/PDMS	35.4 vol%	52.2	2	8–12 Ghz	[141]
NR/CNT	7 wt%	44.2	2	8–12 Ghz	[140]
PBS/CNT	2 wt%	24	2	8–12 Ghz	[124]
CNT/PDMS	2.2 vol%	47	2	8–12 Ghz	[136]
TPU/EG/AG	0.58 vol%	56.3	-	8–12 Ghz	[134]

* PEBA—polyether block amide; CNS—carbon nanostructures; PSS—polystyrene sulfonate; RGC—reduced graphene oxide/single-wall carbon nanotube; PP—polypropylene; BN—boron nitride nanosheet; PPS—polyphenylene sulfide; NR—natural rubber; EG—expanded graphite.

3.4. Layered Structure

The polymer-based EMI shielding composite material with a layered structure contains multiple interfaces, allowing for repeated reflection of electromagnetic radiation, leading to polarization loss and electromagnetic wave absorption loss [142][143]. This layered structure of EMI shielding material can achieve high electromagnetic shielding performance even with a low content of conductive filler, while offering design flexibility. Typically, polymer-based electromagnetic shielding composites with a layered structure exhibit sandwich and gradient configurations, which can be easily prepared using methods like vacuum filtration and deposition [144][145][146]. Due

to their strong absorbing ability, these layered materials find extensive applications in critical fields such as military technology and precision instruments, significantly reducing secondary pollution caused by electromagnetic wave reflection [147][148][149][150]. Yu et al. [151] prepared PI(polyimide)/Ti_3C_2Tx Mxene/AgNW(silver nanowire) composite through electrostatic spinning and a hot-press approach. Wu et al. [152] obtained PPA6@NiM(magnetic PA6 microspheres)/PDMS composite using the solvent coprecipitation method. Chu et al. [153] prepared h-PANI/CNF/Mxene composite films with the alternating vacuum-assisted filtration method. Guo et al. [154] obtained ANF(aramid nanofiber)/AgNW/GN composite films through a vacuum filtration and hot-press approach. They found that the electromagnetic shielding material with a layered structure exhibited a strong absorbing ability, primarily attributed to the formation of a dense conductive network in the core layer of the material and excellent adhesion between the layers [42][151][152][153][154]. **Table 4** shows the recent research of layered-structured electromagnetic shielding materials. Song et al. [155] obtained TPU/MWCNT electromagnetic shielding material with a sandwich structure through the CO_2 foaming method.

Polymer-based electromagnetic shielding composite materials with a layered structure offer significant design freedom, low cost, and strong microwave absorption ability. However, they encounter challenges in actual production [41][156][157]. The bonding of the layers in the layered structure material using physical methods can degrade the compatibility between the layers and may also lead to cracks forming during the bonding process. Consequently, these drawbacks have the potential to restrict the application of multilayer polymer-based electromagnetic shielding materials [43][158].

Table 4. Summary of the research on poly-based electromagnetic shielding composites with layered structure.

Materials *	Filler Loading	EMI SE (dB)	Thickness (mm)	Frequency	Ref.
PI/Ti3C2Tx Mxene/AgNW	20 wt%	79.54	0.15	8–12 Ghz	[151]
PLA/MWCNT	5 vol%	26	1.5	24–40 Ghz	[41]
PPA6@NiM/PDMS	54.9 wt%	39.9	1	8–12 Ghz	[152]
PLLA/GNP/Fe_3O_4	10wt%	41.7	0.4	8–12 Ghz	[156]
CF@(CNT/Fe_3O_4/EP)	0.045 wt%	30.5	2	8–12 Ghz	[157]
h-PANI/CNF/Mxene	8 wt%	35.3	-	8–12 Ghz	[153]
PVDF/$SiBi_{58}$/Co-C	30 vol%	50	2	8–12 Ghz	[148]
EP/LMPA	20 vol%	20	-	8–12 Ghz	[143]
SR/Mxene/Fe_3O_4	21.2 wt%	55.5	2	8–12 Ghz	[147]
CF/GF/PDMS	1 wt%	30	1	8–18 Ghz	[149]
ANF/AgNW/GN	2 vol%	68.3	0.04	8–12 Ghz	[154]

Materials *	Filler Loading	EMI SE (dB)	Thickness (mm)	Frequency	Ref.
NR/MXene/CNT	50 wt%	49.9	0.2	8–12 Ghz	[43]
PEEK/MWCNT	20 wt%	44.5	0.56	8–12 Ghz	[42]
TPU/MWCNT	5 wt%	53.3	2.4	8–12 Ghz	[155]
$NiFe_2O_4$/AgNW/EPM	10 wt%	66.5	2	8–12 Ghz	[159]
MXene/AgNW/MoS_2	10 wt%	86.3	0.03	8–12 Ghz	[160]

* LMPA—low-melting-point alloy; SR—silicone rubber; GF—graphene fiber; PEEK—polyether-ether-ketone.

References

1. Wan, Y.; Xiong, P.; Liu, J.; Feng, F.; Xun, X.; Gama, F.M.; Zhang, Q.; Yao, F.; Yang, Z.; Luo, H.; et al. Ultrathin, Strong, and Highly Flexible Ti3C2Tx MXene/Bacterial Cellulose Composite Films for High-Performance Electromagnetic Interference Shielding. ACS Nano 2021, 15, 8439–8449.
2. Zhan, Y.; Oliviero, M.; Wang, J.; Sorrentino, A.; Buonocore, G.G.; Sorrentino, L.; Lavorgna, M.; Xia, H.; Iannace, S. Enhancing the EMI shielding of natural rubber-based supercritical CO2 foams by exploiting their porous morphology and CNT segregated networks. Nanoscale 2019, 11, 1011–1020.
3. Zhao, B.; Deng, J.; Zhang, R.; Liang, L.; Fan, B.; Bai, Z.; Shao, G.; Park, C.B. Recent Advances on the Electromagnetic Wave Absorption Properties of Ni Based Materials. Eng. Sci. 2018, 3, 5–40.
4. Chen, X.; Wang, W.; Shi, T.; Wu, G.; Lu, Y. One pot green synthesis and EM wave absorption performance of MoS2@nitrogen doped carbon hybrid decorated with ultrasmall cobalt ferrite nanoparticles. Carbon 2020, 163, 202–212.
5. Limthin, D.; Klamchuen, A.; Phromyothin, D. Surface modification of superparamagnetic iron oxide nanoparticles and methyl methacrylate molecularly imprinted polymer for gluten detection. Ferroelectrics 2019, 552, 97–107.
6. Zhang, X.; Zhao, Z.; Xu, J.; Ouyang, Q.; Zhu, C.; Zhang, X.; Zhang, X.; Chen, Y. N-doped carbon nanotube arrays on reduced graphene oxide as multifunctional materials for energy devices and absorption of electromagnetic wave. Carbon 2021, 177, 216–225.
7. Shao, H.; Wen, Z.; Cheng, P.; Sun, N.; Shen, Q.; Zhou, C.; Peng, M.; Yang, Y.; Xie, X.; Sun, X. Multifunctional power unit by hybridizing contact-separate triboelectric nanogenerator, electromagnetic generator and solar cell for harvesting blue energy. Nano Energy 2017, 39, 608–615.
8. Xia, L.; Zhang, Y. An overview of world geothermal power generation and a case study on China—The resource and market perspective. Renew. Sustain. Energy Rev. 2019, 112, 411–423.

9. Joseph, J.; Koroth, A.K.; John, D.A.; Sidpara, A.M.; Paul, J. Highly filled multilayer thermoplastic/graphene conducting composite structures with high strength and thermal stability for electromagnetic interference shielding applications. J. Appl. Polym. Sci. 2019, 136, 47792.
10. Ma, F.; Yuan, N.; Ding, J. The conductive network made up by the reduced graphene nanosheet/polyaniline/polyvinyl chloride. J. Appl. Polym. Sci. 2012, 128, 3870–3875.
11. Singh, S.K.; Akhtar, M.J.; Kar, K.K. Hierarchical Carbon Nanotube-Coated Carbon Fiber: Ultra Lightweight, Thin, and Highly Efficient Microwave Absorber. ACS Appl. Mater. Interfaces 2018, 10, 24816–24828.
12. Wongkasem, N. Electromagnetic pollution alert: Microwave radiation and absorption in human organs and tissues. Electromagn. Biol. Med. 2021, 40, 236–253.
13. Chen, Y.; Yang, Y.; Xiong, Y.; Zhang, L.; Xu, W.; Duan, G.; Mei, C.; Jiang, S.; Rui, Z.; Zhang, K. Porous aerogel and sponge composites: Assisted by novel nanomaterials for electromagnetic interference shielding. Nano Today 2021, 38, 101204.
14. Rajavel, K.; Hu, Y.; Zhu, P.; Sun, R.; Wong, C. MXene/metal oxides-Ag ternary nanostructures for electromagnetic interference shielding. Chem. Eng. J. 2020, 399, 125791.
15. Oh, K.; Hong, S.M.; Seo, Y. Effect of crosslinking reaction on the electromagnetic interference shielding of a Fe-Si-Al alloy (Sendust)/polymer composite at high frequency. Polym. Adv. Technol. 2014, 25, 1366–1370.
16. Choi, H.K.; Lee, A.; Park, M.; Lee, D.S.; Bae, S.; Lee, S.-K.; Lee, S.H.; Lee, T.; Kim, T.-W. Hierarchical Porous Film with Layer-by-Layer Assembly of 2D Copper Nanosheets for Ultimate Electromagnetic Interference Shielding. ACS Nano 2021, 15, 829–839.
17. Zhang, C.-S.; Ni, Q.-Q.; Fu, S.-Y.; Kurashiki, K. Electromagnetic interference shielding effect of nanocomposites with carbon nanotube and shape memory polymer. Compos. Sci. Technol. 2007, 67, 2973–2980.
18. Geetha, S.; Satheesh Kumar, K.K.; Rao, C.R.K.; Vijayan, M.; Trivedi, D.C. EMI shielding: Methods and materials—A review. J. Appl. Polym. Sci. 2009, 112, 2073–2086.
19. Cao, M.-S.; Wang, X.-X.; Cao, W.-Q.; Yuan, J. Ultrathin graphene: Electrical properties and highly efficient electromagnetic interference shielding. J. Mater. Chem. C 2015, 3, 6589–6599.
20. Jiang, X.; Li, S.; He, S.; Bai, Y.; Shao, L. Interface manipulation of CO2–philic composite membranes containing designed UiO-66 derivatives towards highly efficient CO2 capture. J. Mater. Chem. A 2018, 6, 15064–15073.
21. Ye, W.; Xie, M.; Huang, Z.; Wang, H.; Zhou, Q.; Wang, L.; Chen, B.; Wang, H.; Liu, W. Microstructure and tribological properties of in-situ carbide/CoCrFeNiMn high entropy alloy composites synthesized by flake powder metallurgy. Tribol. Int. 2023, 181, 108295.

22. Hua, D.; Liu, X.; Wang, W.; Zhou, Q.; Xia, Q.; Li, S.; Shi, J.; Wang, H. Formation mechanism of hierarchical twins in the CoCrNi medium entropy alloy. J. Mater. Sci. Technol. 2023, 140, 19–32.
23. Ren, Y.; Huang, Z.; Wang, Y.; Zhou, Q.; Yang, T.; Li, Q.; Jia, Q.; Wang, H. Friction-induced rapid amorphization in a wear-resistant (CoCrNi)88Mo12 dual-phase medium-entropy alloy at cryogenic temperature. Compos. Part B Eng. 2023, 263, 110833.
24. Wan, Q.; Hua, K.; Zhou, Z.; Zhang, F.; Wu, H.; Zhou, Q.; Wang, H. Revealing the B addition on tribology performance in TiZrHfTa0.5 refractory high-entropy alloy at ambient and elevated temperature. J. Alloys Compd. 2022, 931, 167521.
25. Luo, D.; Zhou, Q.; Huang, Z.; Li, Y.; Liu, Y.; Li, Q.; He, Y.; Wang, H. Tribological Behavior of High Entropy Alloy Coatings: A Review. Coatings 2022, 12, 1428.
26. Zhang, K.; Gu, X.; Dai, Q.; Yuan, B.; Yan, Y.; Guo, M. Flexible polyaniline-coated poplar fiber composite membranes with effective electromagnetic shielding performance. Vacuum 2019, 170, 108990.
27. Dogan, S.; Kayacan, O.; Goren, A. A lightweight, strength and electromagnetic shielding polymer composite structure for infant carrier strollers. Polym. Compos. 2019, 40, 4559–4572.
28. Tan, Y.-J.; Li, J.; Cai, J.-H.; Tang, X.-H.; Liu, J.-H.; Hu, Z.-Q.; Wang, M. Comparative study on solid and hollow glass microspheres for enhanced electromagnetic interference shielding in polydimethylsiloxane/multi-walled carbon nanotube composites. Compos. Part B Eng. 2019, 177, 107378.
29. Zhang, Y.; Qiu, M.; Yu, Y.; Wen, B.; Cheng, L. A Novel Polyaniline-Coated Bagasse Fiber Composite with Core–Shell Heterostructure Provides Effective Electromagnetic Shielding Performance. ACS Appl. Mater. Interfaces 2016, 9, 809–818.
30. Zhao, H.; Hou, L.; Bi, S.; Lu, Y. Enhanced X-Band Electromagnetic-Interference Shielding Performance of Layer-Structured Fabric-Supported Polyaniline/Cobalt–Nickel Coatings. ACS Appl. Mater. Interfaces 2017, 9, 33059–33070.
31. Wang, Y.; Jing, X. Intrinsically conducting polymers for electromagnetic interference shielding. Polym. Adv. Technol. 2005, 16, 344–351.
32. Sun, F.; Xu, J.; Liu, T.; Li, F.; Poo, Y.; Zhang, Y.; Xiong, R.; Huang, C.; Fu, J. An autonomously ultrafast self-healing, highly colourless, tear-resistant and compliant elastomer tailored for transparent electromagnetic interference shielding films integrated in flexible and optical electronics. Mater. Horiz. 2021, 8, 3356–3367.
33. Nazir, A.; Yu, H.; Wang, L.; Haroon, M.; Ullah, R.S.; Fahad, S.; Naveed, K.-U.-R.; Elshaarani, T.; Khan, A.; Usman, M. Recent progress in the modification of carbon materials and their application in composites for electromagnetic interference shielding. J. Mater. Sci. 2018, 53, 8699–8719.

34. Wang, L.; Qiu, H.; Liang, C.; Song, P.; Han, Y.; Han, Y.; Gu, J.; Kong, J.; Pan, D.; Guo, Z. Electromagnetic Interference Shielding MWCNT-Fe3O4@Ag/Epoxy Nanocomposites with Satisfactory Thermal Conductivity and High Thermal Stability. Carbon 2018, 141, 506–514.
35. Wang, L.; Chen, L.; Song, P.; Liang, C.; Lu, Y.; Qiu, H.; Zhang, Y.; Kong, J.; Gu, J. Fabrication on the annealed Ti3C2Tx MXene/Epoxy nanocomposites for electromagnetic interference shielding application. Compos. Part B Eng. 2019, 171, 111–118.
36. Zhu, N.; Jiang, T.; Zeng, X.; Li, S.; Shen, C.; Zhang, C.; Gong, W.; He, L. High strength and light weight polyamide 6/carbon fiber composite foams for electromagnetic interference shielding. J. Appl. Polym. Sci. 2023, 140, e53818.
37. Li, J.; Zhang, S.; Wang, L.; Liu, X. In Situ Growth of Fe3O4 Nanoparticles in Poly(arylene ether nitrile)/Graphene/Carbon Nanotube Foams for Electromagnetic Interference Shielding. ACS Appl. Nano Mater. 2023, 6, 7802–7813.
38. Huang, B.; Yue, J.; Fan, B.; Tang, X.Z.; Liu, Y.; Huang, X. Constructing hierarchical structure via in situ growth of CNT in SiO2-coated carbon foam for high-performance EMI shielding application. Compos. Sci. Technol. 2022, 222, 109372.
39. Li, X.; Wu, M.; Chen, J.; Zhou, X.; Ren, Q.; Wang, L.; Shen, B.; Zheng, W. A facile and large-scale approach to prepare macroscopic segregated polyether block amides/carbon nanostructures composites with a gradient structure for absorption-dominated electromagnetic shielding with ultra-low reflection. Compos. Commun. 2023, 40, 101628.
40. Chen, C.; Zhao, X.; Ye, L. Low Percolation Threshold and Enhanced Electromagnetic Interference Shielding in Polyoxymethylene/Carbon Nanotube Nanocomposites with Conductive Segregated Networks. Ind. Eng. Chem. Res. 2022, 61, 3962–3972.
41. Bertašius, P.; Plyushch, A.; Macutkevič, J.; Banys, J.; Selskis, A.; Platnieks, O.; Gaidukovs, S. Multilayered Composites with Carbon Nanotubes for Electromagnetic Shielding Application. Polymers 2023, 15, 1053.
42. Wu, T.H.; Mei, X.H.; Liang, L.B.; Ma, Y.M.; Wang, G.B.; Zhang, S.L. Achieving structurally and functionally integrated electromagnetic shielding composites based on polyetheretherketone by sandwich structure. J. Sandw. Struct. Mater. 2021, 24, 484–502.
43. Wu, H.; Zhu, C.; Li, X.; Hu, X.; Xie, H.; Lu, X.; Qu, J.-P. Layer-by-Layer Assembly of Multifunctional NR/MXene/CNTs Composite Films with Exceptional Electromagnetic Interference Shielding Performances and Excellent Mechanical Properties. Macromol. Rapid Commun. 2022, 43, e2200387.
44. Ryu, S.H.; Kim, H.; Park, S.-W.; Kwon, S.J.; Kim, S.; Lim, H.-R.; Park, B.; Lee, S.-B.; Choa, Y.-H. Millimeter-Scale Percolated Polyethylene/Graphene Composites for 5G Electromagnetic Shielding. ACS Appl. Nano Mater. 2022, 5, 8429–8439.

45. Zhang, Y.; Gu, J. A Perspective for Developing Polymer-Based Electromagnetic Interference Shielding Composites. Nano-Micro Lett. 2022, 14, 1–9.
46. Zhao, B.; Hamidinejad, M.; Wang, S.; Bai, P.; Che, R.; Zhang, R.; Park, C.B. Advances in electromagnetic shielding properties of composite foams. J. Mater. Chem. A 2021, 9, 8896–8949.
47. Shukla, V. Review of electromagnetic interference shielding materials fabricated by iron ingredients. Nanoscale Adv. 2019, 1, 1640–1671.
48. Sankaran, S.; Deshmukh, K.; Ahamed, M.B.; Khadheer Pasha, S.K. Recent advances in electromagnetic interference shielding properties of metal and carbon filler reinforced flexible polymer composites: A review. Compos. Part A Appl. Sci. Manuf. 2018, 114, 49–71.
49. Wang, L.; Song, P.; Lin, C.-T.; Kong, J.; Gu, J. 3D Shapeable, Superior Electrically Conductive Cellulose Nanofibers/Ti3C2Tx MXene Aerogels/Epoxy Nanocomposites for Promising EMI Shielding. Research 2020, 2020, 4093732.
50. Ji, H.; Zhao, R.; Zhang, N.; Jin, C.; Lu, X.; Wang, C. Lightweight and flexible electrospun polymer nanofiber/metal nanoparticle hybrid membrane for high-performance electromagnetic interference shielding. NPG Asia Mater. 2018, 10, 749–760.
51. Wang, H.; Li, S.; Liu, M.; Li, J.; Zhou, X. Review on Shielding Mechanism and Structural Design of Electromagnetic Interference Shielding Composites. Macromol. Mater. Eng. 2021, 306, 2100032.
52. Omana, L.; Chandran, A.; John, R.E.; Wilson, R.; George, K.C.; Unnikrishnan, N.V.; Varghese, S.S.; George, G.; Simon, S.M.; Paul, I. Recent Advances in Polymer Nanocomposites for Electromagnetic Interference Shielding: A Review. ACS Omega 2022, 7, 25921–25947.
53. Abdi, M.M.; Kassim, A.B.; Ekramul Mahmud, H.N.M.; Yunus, W.M.M.; Talib, Z.A. Electromagnetic Interference Shielding Effectiveness of New Conducting Polymer Composite. J. Macromol. Sci. Part A 2009, 47, 71–75.
54. Rathi, V.; Panwar, V. Electromagnetic Interference Shielding Analysis of Conducting Composites in Near- and Far-Field Region. IEEE Trans. Electromagn. Compat. 2018, 60, 1795–1801.
55. Xu, W.; Pan, Y.-F.; Wei, W.; Wang, G.-S. Nanocomposites of Oriented Nickel Chains with Tunable Magnetic Properties for High-Performance Broadband Microwave Absorption. ACS Appl. Energy Mater. 2018, 1, 1116–1123.
56. Gargama, H.; Thakur, A.K.; Chaturvedi, S.K. Polyvinylidene fluoride/nanocrystalline iron composite materials for EMI shielding and absorption applications. J. Alloys Compd. 2016, 654, 209–215.
57. Tian, D.; Xu, Y.; Wang, Y.; Lei, Z.; Lin, Z.; Zhao, T.; Hu, Y.; Sun, R.; Wong, C.-P. In-Situ Metallized Carbon Nanotubes/Poly(Styrene-Butadiene-Styrene) (CNTs/SBS) Foam for Electromagnetic Interference Shielding. Chem. Eng. J. 2021, 420, 130482.

58. Chen, M.; Zhang, L.; Duan, S.; Jing, S.; Jiang, H.; Luo, M.; Li, C. Highly conductive and flexible polymer composites with improved mechanical and electromagnetic interference shielding performances. Nanoscale 2014, 6, 3796–3803.
59. Kamkar, M.; Ghaffarkhah, A.; Hosseini, E.; Amini, M.; Ghaderi, S.; Arjmand, M. Multilayer polymeric nanocomposites for electromagnetic interference shielding: Fabrication, mechanisms, and prospects. New J. Chem. 2021, 45, 21488–21507.
60. Kumar, R.; Choudhary, H.K.; Pawar, S.P.; Bose, S.; Sahoo, B. Carbon encapsulated nanoscale iron/iron-carbide/graphite particles for EMI shielding and microwave absorption. Phys. Chem. Chem. Phys. 2017, 19, 23268–23279.
61. Manna, K.; Srivastava, S.K. Tuning of Shells in Trilaminar Core@Shell Nanocomposites in Controlling Electromagnetic Interference through Switching of the Shielding Mechanism. Langmuir 2020, 36, 4519–4531.
62. Ayub, S.; Guan, B.H.; You, K.Y. Electromagnetic Interference Shielding Mechanisms of MMG@PVDF Composites for a Broadband Frequency Range. Mater. Today Commun. 2023, 35, 106273.
63. Han, T.; Luo, R. Effect of carbon nanotubes on the electromagnetic shielding properties of SiC f /SiC composites. J. Alloys Compd. 2018, 745, 90–99.
64. Hu, X.-S.; Shen, Y.; Lu, L.-S.; Xu, J.; Zhen, J.-J. Enhanced electromagnetic interference shielding effectiveness of ternary PANI/CuS/RGO composites. J. Mater. Sci. Mater. Electron. 2017, 28, 6865–6872.
65. Zhao, Z.J.; Zhang, B.Y.; Du, Y.; Hei, Y.W.; Yi, X.S.; Shi, F.H.; Xian, G.J. MWCNT modified structure-conductive composite and its electromagnetic shielding behavior. Compos. Part B Eng. 2017, 130, 21–27.
66. Bera, R.; Das, A.K.; Maitra, A.; Paria, S.; Karan, S.K.; Khatua, B.B. Salt leached viable porous Fe3O4 decorated polyaniline—SWCNH/PVDF composite spectacles as an admirable electromagnetic shielding efficiency in extended Ku-band region. Compos. Part B Eng. 2017, 129, 210–220.
67. Liang, J.; Wang, Y.; Huang, Y.; Ma, Y.; Liu, Z.; Cai, J.; Zhang, C.; Gao, H.; Chen, Y. Electromagnetic interference shielding of graphene/epoxy composites. Carbon 2009, 47, 922–925.
68. Byeon, J.H.; Kim, J.-W. Aerosol based fabrication of a Cu/polymer and its application for electromagnetic interference shielding. Thin Solid Film. 2011, 520, 1048–1052.
69. Okazaki, Y.; Ueno, K. Magnetic shielding by soft magnetic materials in alternating magnetic field. J. Magn. Magn. Mater. 1992, 112, 192–194.

70. Gahlout, P.; Choudhary, V. EMI shielding response of polypyrrole-MWCNT/polyurethane composites. Synth. Met. 2020, 266, 116414.
71. Shakir, M.F.; Abdul Rashid, I.; Tariq, A.; Nawab, Y.; Afzal, A.; Nabeel, M.; Naseem, A.; Hamid, U. EMI Shielding Characteristics of Electrically Conductive Polymer Blends of PS/PANI in Microwave and IR Region. J. Electron. Mater. 2020, 49, 1660–1665.
72. Li, X.; Xu, T.; Cao, W.; Wang, M.; Chen, F.; Jin, L.; Song, N.; Sun, S.; Ding, P. Graphene/carbon fiber network constructed by co-carbonization strategy for functional integrated polyimide composites with enhanced electromagnetic shielding and thermal conductive properties. Chem. Eng. J. 2023, 464, 142595.
73. Meher, D.; Suman, N.; Karna, N.; Sahoo, B.P. Development of Poly (vinylidene fluoride) and Polyaniline blend with high dielectric permittivity, excellent electromagnetic shielding effectiveness and Ultra low optical energy band gap: Effect of ionic liquid and temperature. Polymer 2019, 181, 121759.
74. Acharya, S.; Datar, S. Wideband (8–18 GHz) microwave absorption dominated electromagnetic interference (EMI) shielding composite using copper aluminum ferrite and reduced graphene oxide in polymer matrix. J. Appl. Phys. 2020, 128, 104902.
75. Li, J.; Wang, Y.; Yue, T.-N.; Gao, Y.-N.; Shi, Y.-D.; Shen, J.-B.; Wu, H.; Wang, M. Robust electromagnetic interference shielding, joule heating, thermal conductivity, and anti-dripping performances of polyoxymethylene with uniform distribution and high content of carbon-based nanofillers. Compos. Sci. Technol. 2021, 206, 108681.
76. Li, T.; Zhao, G.; Wang, G. Effect of preparation methods on electrical and electromagnetic interference shielding properties of PMMA/MWCNT nanocomposites. Polym. Compos. 2018, 40, E1786–E1800.
77. Chung, D.D.L. Carbon materials for structural self-sensing, electromagnetic shielding and thermal interfacing. Carbon 2012, 50, 3342–3353.
78. Gupta, S.; Tai, N.-H. Carbon Materials and Their Composites for Electromagnetic Interference Shielding Effectiveness in X-band. Carbon 2019, 152, 159–187.
79. Khodiri, A.A.; Al-Ashry, M.Y.; El-Shamy, A.G. Novel hybrid nanocomposites based on polyvinyl alcohol/graphene/magnetite nanoparticles for high electromagnetic shielding performance. J. Alloys Compd. 2020, 847, 156430.
80. Zhang, H.; Heng, Z.; Zhou, J.; Shi, Y.; Chen, Y.; Zou, H.; Liang, M. In-situ co-continuous conductive network induced by carbon nanotubes in epoxy composites with enhanced electromagnetic interference shielding performance. Chem. Eng. J. 2020, 398, 125559.
81. Serrato, V.M.; Padilla, V.; Jones, D.; Herrera, S.; Campos, L.; Serrato, I.; Foltz, H.; Lozano, K. Electromagnetic interference shielding effectiveness of compression molded carbon nanofiber-

reinforced polyvinylidene difluoride film. Polym. Compos. 2022, 44, 592–608.

82. Mohsina, T.; Manohara, S.R.; Siddlingeshwar, B.; Narasimha, R.; Muhammad, F.; Khadke, U.V. Anticorrosion and electromagnetic interference shielding performance of bifunctional PEDOT-graphene nanocomposites. Diam. Relat. Mater. 2023, 132, 109690.
83. Vineeta, S.; Sanjeev, K.S. Reduced graphene oxide/PdNi/poly(ethylene-co-vinyl acetate) nanocomposites for electromagnetic interference shielding. Mater. Chem. Phys. 2021, 276, 125418.
84. Zhao, Y.; Hou, J.; Bai, Z.; Yang, Y.; Guo, X.; Cheng, H.; Zhao, Z.; Zhang, X.; Chen, J.; Shen, C. Facile preparation of lightweight PE/PVDF/Fe3O4/CNTs nanocomposite foams with high conductivity for efficient electromagnetic interference shielding. Compos. Part A Appl. Sci. Manuf. 2020, 139, 106095.
85. Kuang, T.; Chang, L.; Chen, F.; Sheng, Y.; Fu, D.; Peng, X. Facile preparation of lightweight high-strength biodegradable polymer/multi-walled carbon nanotubes nanocomposite foams for electromagnetic interference shielding. Carbon 2016, 105, 305–313.
86. Zeng, Q.; Du, Z.; Qin, C.; Wang, Y.; Liu, C.; Shen, C. Enhanced thermal, mechanical and electromagnetic interference shielding properties of graphene nanoplatelets-reinforced poly(lactic acid)/poly(ethylene oxide) nanocomposites. Mater. Today Commun. 2020, 25, 101632.
87. Zhang, H.; Zhang, G.; Tang, M.; Zhou, L.; Li, J.; Fan, X.; Shi, X.; Qin, J. Synergistic effect of carbon nanotube and graphene nanoplates on the mechanical, electrical and electromagnetic interference shielding properties of polymer composites and polymer composite foams. Chem. Eng. J. 2018, 353, 381–393.
88. Ni, J.; Zhan, R.; Qiu, J.; Fan, J.; Dong, B.; Guo, Z. Multi-interfaced graphene aerogel/polydimethylsiloxane metacomposites with tunable electrical conductivity for enhanced electromagnetic interference shielding. J. Mater. Chem. C 2020, 8, 11748–11759.
89. Chakraborty, T.; Debnath, T.; Bhowmick, S.; Bandyopadhyay, A.; Karmakar, A.; Das, S.; Mahapatra, A.S.; Sutradhar, S. Enhancement of EMI shielding effectiveness of flexible Co2U-type hexaferrite (Ba4Co2Fe36O60)-poly(vinylidene fluoride) heterostructure composite materials: An improved radar absorbing material to combat against electromagnetic pollution. J. Appl. Phys. 2020, 128, 095301.
90. Cheng, Z.; Cao, Y.; Wang, R.; Xia, L.; Ma, S.; Li, Z.; Cai, Z.; Zhang, Z.; Huang, Y. Hierarchical Surface Engineering of Carbon Fiber for Enhanced Composites Interfacial Properties and Microwave Absorption Performance. Carbon 2021, 185, 669–680.
91. Schmitz, D.P.; Silva, T.I.; Ramoa, S.D.A.S.; Barra, G.M.O.; Pegoretti, A.; Soares, B.G. Hybrid composites of ABS with carbonaceous fillers for electromagnetic shielding applications. J. Appl. Polym. Sci. 2018, 135, 46546.

92. George, G.; Simon, S.M.; Prakashan, V.P.; Sajna, M.S.; Faisal, M.; Chandran, A.; Wilson, R.; Biju, P.R.; Joseph, C.; Unnikrishnan, N.V. Morphological, dielectric, tunable electromagnetic interference shielding and thermal characteristics of multiwalled carbon nanotube incorporated polymer nanocomposites: A facile, environmentally benign and cost effective approach realized via polymer latex/waterborne polymer as matrix. Polym. Compos. 2017, 39, E1169–E1183.
93. Zhang, Y.; Yang, Z.; Yu, Y.; Wen, B.; Liu, Y.; Qiu, M. Tunable Electromagnetic Interference Shielding Ability in a One-Dimensional Bagasse Fiber/Polyaniline Heterostructure. ACS Appl. Energy Mater. 2019, 1, 737–745.
94. Ankur, K.; Palash, D.; Sangit, P.; Krishnendu, N.; Suman Kumar, G.; Narayan, C.D. Preferential localization of conductive filler in ethylene-co-methyl acrylate/thermoplastic polyolefin polymer blends to reduce percolation threshold and enhanced electromagnetic radiation shielding over K band region. Polym. Compos. 2022, 44, 1603–1616.
95. Wang, Y.; Yang, C.; Xin, Z.; Luo, Y.; Wang, B.; Feng, X.; Mao, Z.; Sui, X. Poly(lactic acid)/carbon nanotube composites with enhanced electrical conductivity via a two-step dispersion strategy. Compos. Commun. 2022, 30, 101087.
96. Raju, P.; Rani, G.N.; Kumar, S.U.; Andrews, J.; Raju, K.C.J. Ultrasonically induced in situ polymerization of PANI-SWCNT nanocomposites for electromagnetic shielding applications. J. Mater. Sci. Mater. Electron. 2022, 33, 5138–5148.
97. Chen, K.; Feng, Y.; Shi, Y.; Wang, H.; Fu, L.; Liu, M.; Lv, Y.; Yang, F.; Yu, B.; Liu, M.; et al. Flexible and fire safe sandwich structured composites with superior electromagnetic interference shielding properties. Compos. Part A Appl. Sci. Manuf. 2022, 160, 107070.
98. Wan, Y.-J.; Zhu, P.-L.; Yu, S.-H.; Sun, R.; Wong, C.-P.; Liao, W.-H. Anticorrosive, Ultralight, and Flexible Carbon-Wrapped Metallic Nanowire Hybrid Sponges for Highly Efficient Electromagnetic Interference Shielding. Small 2018, 14, 1800534.
99. Zeng, Z.; Zhang, Y.; Ma, X.; Shahabadi, S.I.S.; Che, B.; Wang, P.; Lu, X. Biomass-based honeycomb-like architectures for preparation of robust carbon foams with high electromagnetic interference shielding performance. Carbon 2018, 140, 227–236.
100. Sun, Y.; Luo, S.; Sun, H.; Zeng, W.; Ling, C.; Chen, D.; Chan, V.; Liao, K. Engineering closed-cell structure in lightweight and flexible carbon foam composite for high-efficient electromagnetic interference shielding. Carbon 2018, 136, 299–308.
101. Dhakate, S.R.; Subhedar, K.M.; Singh, B.P. Polymer nanocomposite foam filled with carbon nanomaterials as an efficient electromagnetic interference shielding material. RSC Adv. 2015, 5, 43036–43057.
102. Li, M.; Xu, Q.; Jiang, W.; Farooq, A.; Qi, Y.; Liu, L. Preparation and Investigation of Fe3O4@rGO/CNF Foams for Electromagnetic Interference Shielding. Fibers Polym. 2023, 24,

771–778.

103. Xu, Y.; Li, Y.; Hua, W.; Zhang, A.; Bao, J. Light-Weight Silver Plating Foam and Carbon Nanotube Hybridized Epoxy Composite Foams with Exceptional Conductivity and Electromagnetic Shielding Property. ACS Appl. Mater. Interfaces 2016, 8, 24131–24142.
104. Ling, J.; Zhai, W.; Feng, W.; Shen, B.; Zhang, J.; Zheng, W.G. Facile Preparation of Lightweight Microcellular Polyetherimide/Graphene Composite Foams for Electromagnetic Interference Shielding. ACS Appl. Mater. Interfaces 2013, 5, 2677–2684.
105. Oraby, H.; Naeem, I.; Darwish, M.; Senna, M.H.; Tantawy, H.R. Electromagnetic interference shielding of thermally exfoliated graphene/polyurethane composite foams. J. Appl. Polym. Sci. 2022, 139, 53008.
106. Chen, J.; Jiang, W.J.; Zeng, Z.; Sun, D.X.; Qi, X.D.; Yang, J.H.; Wang, Y. Multifunctional shape memory foam composites integrated with tunable electromagnetic interference shielding and sensing. Chem. Eng. J. 2023, 466, 143373.
107. Li, Z.; Sun, Y.; Zhou, B.; Feng, Y.; Liu, C.; Shen, C. Flexible thermoplastic polyurethane/MXene foams for compressible electromagnetic interference shielding. Mater. Today Phys. 2023, 32, 101017.
108. Liu, H.; Zhu, Z.; Tian, N.; Li, Y.; You, C.; Islam, S.M. Synergistically-enhanced flexible electromagnetic interference shielding nanocomposites. Appl. Surf. Sci. 2023, 628, 157379.
109. Lee, C.W.; Lin, C.H.; Wang, L.Y.; Lee, Y.H. Developing sustainable and recyclable high-efficiency electromagnetic interference shielding nanocomposite foams from the upcycling of recycled poly(ethylene terephthalate). Chem. Eng. J. 2023, 468, 143447.
110. Oraby, H.; Naeem, I.; Darwish, M.; Senna, M.H.; Tantawy, H.R. Optimization of electromagnetic shielding and mechanical properties of reduced graphene oxide/polyurethane composite foam. Polym. Eng. Sci. 2022, 62, 3075–3087.
111. Wang, X.; Wang, G.; He, G.; Liao, X.; Song, P.; Zou, F.; Liu, S.; Luo, Y.; Li, G. Fabrication of lightweight flexible thermoplastic polyurethane/multiwalled carbon nanotubes composite foams for adjustable frequency-selective electromagnetic interference shielding by supercritical carbon dioxide. J. Supercrit. Fluids 2022, 188, 105675.
112. Dun, D.; Luo, J.; Wang, M.; Wang, X.; Zhou, H.; Wang, X.; Wen, B.; Zhang, Y. Electromagnetic Interference Shielding Foams Based on Poly(vinylidene fluoride)/Carbon Nanotubes Composite. Macromol. Mater. Eng. 2021, 306, 2100468.
113. Zou, F.; Chen, J.; Liao, X.; Song, P.; Li, G. Efficient electrical conductivity and electromagnetic interference shielding performance of double percolated polymer composite foams by phase coarsening in supercritical CO2. Compos. Sci. Technol. 2021, 213, 108895.

114. Shen, Y.; Lin, Z.; Liu, X.; Zhao, T.; Zhu, P.; Zeng, X.; Hu, Y.; Sun, R.; Wong, C.-P. Robust and flexible silver-embedded elastomeric polymer/carbon black foams with outstanding electromagnetic interference shielding performance. Compos. Sci. Technol. 2021, 213, 108942.
115. Luo, J.; Yin, D.; Yu, K.; Zhou, H.; Wen, B.; Wang, X. Facile Fabrication of PBS/CNTs Nanocomposite Foam for Electromagnetic Interference Shielding. ChemPhysChem 2022, 23, 202100778.
116. Kim, E.; Zhang, H.; Lee, J.-H.; Chen, H.; Zhang, H.; Javed, M.H.; Shen, X.; Kim, J.-K. MXene/polyurethane auxetic composite foam for electromagnetic interference shielding and impact attenuation. Compos. Part A Appl. Sci. Manuf. 2021, 147, 106430.
117. Liang, S.; Qin, Y.; Gao, W.; Wang, M. A lightweight polyurethane-carbon microsphere composite foam for electromagnetic shielding. e-Polymers 2022, 22, 223–233.
118. Wang, P.; Yang, L.; Ling, J.; Song, J.; Song, T.; Chen, X.; Gao, S.; Feng, S.; Ding, Y.; Murugadoss, V.; et al. Frontal ring-opening metathesis polymerized polydicyclopentadiene carbon nanotube/graphene aerogel composites with enhanced electromagnetic interference shielding. Adv. Compos. Hybrid Mater. 2022, 5, 2066–2077.
119. Xia, B.; Zhang, X.; Jiang, J.; Wang, Y.; Li, T.; Wang, Z.; Chen, M.; Liu, T.; Dong, W. Facile preparation of high strength, lightweight and thermal insulation Polyetherimide/Ti3C2Tx MXenes/Ag nanoparticles composite foams for electromagnetic interference shielding. Compos. Commun. 2021, 29, 101028.
120. Bai, Y.A.; Wei, X.; Dun, D.; Bai, S.; Zhou, H.; Wen, B.; Wang, X.; Hu, J. Lightweight poly(vinylidene fluoride) based quaternary nanocomposite foams with efficient and tailorable electromagnetic interference shielding properties. Polym. Compos. 2023, 44, 1951–1966.
121. Bai, Y.A.; Zheng, K.; Cui, W.; Luo, J.; Zhou, H.; Wang, X.; Wen, B.; Xing, Q. Electromagnetic shielding performance of acrylonitrile-butadiene-styrene/CNTs composite foams with different cell structures. J. Supercrit. Fluids 2022, 186, 105608.
122. Göldel, A.; Kasaliwal, G.; Pötschke, P. Selective Localization and Migration of Multiwalled Carbon Nanotubes in Blends of Polycarbonate and Poly(styrene-acrylonitrile). Macromol. Rapid Commun. 2009, 30, 423–429.
123. Grady, B.P. Recent Developments Concerning the Dispersion of Carbon Nanotubes in Polymers. Macromol. Rapid Commun. 2009, 31, 247–257.
124. Liu, Y.; He, H.; He, G.; Zhao, J.; Yang, Y.; Tian, G. Segregated polylactide/poly(butylene adipate-co-terephthalate)/MWCNTs nanocomposites with excellent electrical conductivity and electromagnetic interference shielding. J. Appl. Polym. Sci. 2021, 139, 51668.
125. Jia, L.-C.; Yan, D.-X.; Cui, C.-H.; Ji, X.; Li, Z.-M. A Unique Double Percolated Polymer Composite for Highly Efficient Electromagnetic Interference Shielding. Macromol. Mater. Eng. 2016, 301,

1232–1241.

126. Zhang, K.; Li, G.-H.; Feng, L.-M.; Wang, N.; Guo, J.; Sun, K.; Yu, K.-X.; Zeng, J.-B.; Li, T.; Guo, Z.; et al. Ultralow percolation threshold and enhanced electromagnetic interference shielding in poly(L-lactide)/multi-walled carbon nanotube nanocomposites with electrically conductive segregated networks. J. Mater. Chem. C 2017, 5, 9359–9369.
127. Zhou, J.; Liu, C.; Xia, L.; Wang, L.; Qi, C.; Zhang, G.; Tan, Z.; Ren, B.; Yuan, B. Bridge-graphene connecting polymer composite with a distinctive segregated structure for simultaneously improving electromagnetic interference shielding and flame-retardant properties. Colloids Surf. A Physicochem. Eng. Asp. 2022, 661, 130853.
128. Mei, X.; Zhao, Y.; Jiang, H.; Gao, T.; Huang, Z.X.; Qu, J.P. Multifunctional starch/carbon nanotube composites with segregated structure: Electrical conductivity, electromagnetic interference shielding effectiveness, thermal conductivity, and electro-thermal conversion. J. Appl. Polym. Sci. 2023, 2023, e53904.
129. Navid, K.; Amir Hosein Ahmadian, H.; Parisa, N.; Jian, L.; Abbas, S.M.; Mohammad, A. Highly conductive polystyrene/carbon Nanotube/PEDOT:PSS nanocomposite with segregated structure for electromagnetic interference shielding. Carbon 2023, 212, 118104.
130. Tian, G.; He, H.; Xu, M.; Liu, Y.; Gao, Q.; Zhu, Z. Ultralow percolation threshold biodegradable PLA/PBS/MWCNTs with segregated conductive networks for high-performance electromagnetic interference shielding applications. J. Appl. Polym. Sci. 2022, 140, e53558.
131. Xiong, Y.; Pei, H.; Lv, Q.; Chen, Y. A Facile Fabrication of PA12/CNTs Nanocomposites with Enhanced Three-Dimensional Segregated Conductive Networks and Electromagnetic Interference Shielding Property through Selective Laser Sintering. ACS Omega 2022, 7, 4293–4304.
132. Zhang, Q.; Cui, J.; Zhao, S.; Gao, A.; Zhang, G.; Yan, Y. Regulation binary electromagnetic filler networks in segregated poly(vinylidenefluoride) composite for absorption-dominated electromagnetic interference shielding. J. Appl. Polym. Sci. 2023, 140, e53650.
133. Wu, B.; Zhu, K.; Wen, X.; Li, M.; Yang, Y.; Yang, J. Fe3O4@PA6/MWCNT composites with multiple gradient segregated structures for electromagnetic shielding with low reflection. J. Appl. Polym. Sci. 2022, 139, 52085.
134. Yang, J.; Chen, Y.; Liu, C.; Wang, H.; Yan, X.; Chai, X.; Chen, Z.; Xia, Y.; Gao, H.; Zhang, H.; et al. Constructing 3D expanded graphite-silver segregated network structure for ultra-efficient EMI shielding and low reflection. J. Mater. Res. Technol. 2023, 23, 5115–5126.
135. Wang, X.; Smith, P.; Qiang, Z.; Guan, Q.; You, Z.; Ye, C.; Zhu, M. Fire-retardant, self-extinguishing multiblock poly(esterimide)s/graphene composites with segregated structure for electromagnetic interference shielding. Compos. Part A Appl. Sci. Manuf. 2022, 163, 107262.

136. Ma, R.-Y.; Yi, S.-Q.; Li, J.; Zhang, J.-L.; Sun, W.-J.; Jia, L.-C.; Yan, D.-X.; Li, Z.-M. Highly efficient electromagnetic interference shielding and superior mechanical performance of carbon nanotube/polydimethylsiloxane composite with interface-reinforced segregated structure. Compos. Sci. Technol. 2022, 232, 109874.

137. Pang, H.; Xu, L.; Yan, D.X.; Li, Z.M. Conductive polymer composites with segregated structures. Prog. Polym. Sci. 2014, 39, 1908–1933.

138. Yu, W.-C.; Xu, J.-Z.; Wang, Z.-G.; Huang, Y.-F.; Yin, H.-M.; Xu, L.; Chen, Y.-W.; Yan, D.-X.; Li, Z.-M. Constructing highly oriented segregated structure towards high-strength carbon nanotube/ultrahigh-molecular-weight polyethylene composites for electromagnetic interference shielding. Compos. Part A Appl. Sci. Manuf. 2018, 110, 237–245.

139. Zhang, L.; Yang, S.; Peng, L.; Zhong, K.; Chen, Y. Optimized Properties in Multifunctional Polyphenylene Sulfide Composites via Graphene Nanosheets/Boron Nitride Nanosheets Dual Segregated Structure under High Pressure. Nanomaterials 2022, 12, 3543.

140. Xie, Z.; Cai, Y.; Zhan, Y.; Meng, Y.; Li, Y.; Xie, Q.; Xia, H. Thermal insulating rubber foams embedded with segregated carbon nanotube networks for electromagnetic shielding applications. Chem. Eng. J. 2022, 435, 135118.

141. Yang, D.; Tao, J.-R.; Yang, Y.; He, Q.-M.; Weng, Y.-X.; Fei, B.; Wang, M. Effect interfacial size and multiple interface on electromagnetic shielding of silicon rubber/carbon nanotube composites with mixing segregated particles. Compos. Struct. 2022, 292, 115668.

142. Wang, Y.; Cheng, X.-D.; Song, W.-L.; Ma, C.-J.; Bian, X.-M.; Chen, M. Hydro-sensitive sandwich structures for self-tunable smart electromagnetic shielding. Chem. Eng. J. 2018, 344, 342–352.

143. Zhang, P.; Tian, R.; Zhang, X.; Ding, X.; Wang, Y.; Xiao, C.; Zheng, K.; Liu, X.; Chen, L.; Tian, X. Electromagnetic interference shielding epoxy composites with satisfactory thermal conductivity and electrical insulation performance enabled by low-melting-point alloy layered structure. Compos. Part B Eng. 2022, 232, 109611.

144. Sheng, A.; Ren, W.; Yang, Y.; Yan, D.-X.; Duan, H.; Zhao, G.; Liu, Y.; Li, Z.-M. Multilayer WPU conductive composites with controllable electro-magnetic gradient for absorption-dominated electromagnetic interference shielding. Compos. Part A Appl. Sci. Manuf. 2019, 129, 105692.

145. Li, Y.; Shen, B.; Yi, D.; Zhang, L.; Zhai, W.; Wei, X.; Zheng, W. The influence of gradient and sandwich configurations on the electromagnetic interference shielding performance of multilayered thermoplastic polyurethane/graphene composite foams. Compos. Sci. Technol. 2017, 138, 209–216.

146. Park, K.; Lee, S.; Kim, C.; Han, J. Fabrication and electromagnetic characteristics of electromagnetic wave absorbing sandwich structures. Compos. Sci. Technol. 2006, 66, 576–584.

147. Li, H.; Ru, X.; Song, Y.; Wang, H.; Yang, C.; Zheng, S.; Gong, L.; Zhang, X.; Duan, H.; Liu, Z.; et al. Flexible Sandwich-Structured Silicone Rubber/MXene/Fe3O4 Composites for Tunable Electromagnetic Interference Shielding. Ind. Eng. Chem. Res. 2022, 61, 11766–11776.

148. Wang, H.; Bi, H.; Liang, D.; Gui, X.; Ding, X.; Zhang, X.; Gao, J.; Zi, Z. Absorption-dominated electromagnetic shielding and excellent thermal conduction properties of poly(vinylidene fluoride)/SnBi58/Co-C composites with layered structure. J. Alloys Compd. 2022, 921, 165998.

149. Xu, L.; Wan, S.; Heng, Y.; Wang, S.; Yang, J.; Dong, Y.; Fu, Y.; Ni, Q. Double layered design for electromagnetic interference shielding with ultra-low reflection features: PDMS including carbon fibre on top and graphene on bottom. Compos. Sci. Technol. 2022, 231, 109797.

150. Zhou, Q.; Luo, D.; Hua, D.; Ye, W.; Li, S.; Zou, Q.; Chen, Z.; Wang, H. Design and characterization of metallic glass/graphene multilayer with excellent nanowear properties. Friction 2022, 10, 1913–1926.

151. Zhang, Y.; Gao, Q.; Sheng, X.; Zhang, S.; Chen, J.; Ma, Y.; Qin, J.; Zhao, Y.; Shi, X.; Zhang, G. Flexible, robust, sandwich structure polyimide composite film with alternative MXene and Ag NWs layers for electromagnetic interference shielding. J. Mater. Sci. Technol. 2023, 159, 194–203.

152. Wu, B.; Yu, Y.; Zhu, K.; Yang, Y.; Wen, X.; Liu, R.; Zhu, H.; Huang, J. Efficient Electromagnetic Interference Shielding of PPA6@NiM/PDMS Composites with Porous and Asymmetric Gradient Structures. ACS Appl. Polym. Mater. 2023, 5, 4789–4798.

153. Chu, Q.; Tao, W.; Lin, H.; Ma, M.; Chen, S.; Shi, Y.; He, H.; Wang, X. Well-designed structure of sandwich-like composite films based on hollow polyaniline and MXene with enhanced electromagnetic wave absorption. Ind. Crops Prod. 2023, 194, 116299.

154. Guo, D.; Huo, Y.; Mu, C.; Wang, B.; Xiang, J.; Nie, A.; Zhai, K.; Xue, T.; Wen, F.; Liu, Z. Flexible aramid nanofiber/Ag nanowires/graphene nanosheets composite films with sandwich structure for high-performance electromagnetic interference shielding and Joule heating. J. Alloys Compd. 2022, 923, 166401.

155. Song, P.; Liao, X.; Zou, F.; Wang, X.; Liu, F.; Liu, S.; Li, G. Frequency-adjustable electromagnetic interference shielding performance of sandwich-structured conductive polymer composites by selective foaming and tunable filler dispersion. Compos. Commun. 2022, 34, 101264.

156. Gu, T.; Zeng, Z.; Wu, S.; Sun, D.X.; Zhao, C.S.; Wang, Y. Poly(L-lactic acid)/graphene composite films with asymmetric sandwich structure for thermal management and electromagnetic interference shielding. Chem. Eng. J. 2023, 466, 143190.

157. Zhang, C.; Bi, L.; Shi, S.; Wang, H.; Zhang, D.; He, Y.; Li, W. Two-Steps Method to Prepare Multilayer Sandwich Structure Carbon Fiber Composite with Thermal and Electrical Anisotropy and Electromagnetic Interference Shielding. Materials 2023, 16, 680.

158. Xia, Q.; Zhang, Z.; Chu, H.; Liu, Y.; Leng, J. Research on high electromagnetic interference shielding effectiveness of a foldable buckypaper/polyacrylonitrile composite film via interface reinforcing. Compos. Part A Appl. Sci. Manuf. 2018, 113, 132–140.

159. Liu, F.; Wei, Z.; Hu, X.; Cai, Y.; Chen, Z.; Yang, C.; Zhan, Y.; Xia, H. Asymmetric segregated network design of ultralight and thermal insulating polymer composite foams for green electromagnetic interference shielding. Compos. Commun. 2022, 38, 101492.

160. Xing, Y.; Wan, Y.; Wu, Z.; Wang, J.; Jiao, S.; Liu, L. Multilayer Ultrathin MXene@AgNW@MoS2 Composite Film for High-Efficiency Electromagnetic Shielding. ACS Appl. Mater. Interfaces 2023, 15, 5787–5797.